Effect of Ambient-Temperature and High-Temperature Electron-Beam Radiation on the Structural, Thermal, Mechanical, and Dynamic Mechanical Properties of Injection-Molded Polyamide-6,6

Rajatendu Sengupta,[1] S. Sabharwal,[2] V. K. Tikku,[3] Alok K. Somani,[4] Tapan K. Chaki,[1] Anil K. Bhowmick[1]

[1]*Rubber Technology Centre, Indian Institute of Technology, Kharagpur 721302, India*
[2]*Radiation Technology Development Section, Bhabha Atomic Research Center, Trombay, Mumbai 400085, India*
[3]*NICCO Corporation, Ltd. (Cable Division), Athpur Works, 24 Parganas, Athpur 743128, India*
[4]*Black Burn & Co., Ltd., P.O. Raipur, 24 Parganas, Maheshtala 743352, India*

Received 3 November 2004; accepted 21 March 2005
DOI 10.1002/app.22689
Published online in Wiley InterScience (www.interscience.wiley.com).

ABSTRACT: Electron-beam irradiation of injection-molded specimens of polyiminohexamethyleneiminoadipoyl (better known as polyamide-6,6) was carried out in air at ambient temperature (303 K) and a high temperature (393 K). Most of the irradiated specimens were tensile dumbbells, although a few were cylinders for compressive stress relaxation testing. A few representative samples were dipped in triallyl cyanurate (TAC) solution before ambient-temperature irradiation. The gel content of the specimens increased with radiation dose and the temperature of irradiation. Moreover, the TAC-treated specimens showed an increase in gel content over the neat specimens irradiated at the same dose levels. Wide-angle X-ray scattering and differential scanning calorimetry studies revealed that the crystallinity decreased with increasing radiation dose. Irradiation at the high temperature and treatment with TAC further decreased the crystallinity compared to irradiation at ambient temperature. As determined from compressive stress relaxation and mechanical and dynamic mechanical properties, the optimized radiation dose for ambient-temperature radiation was 200 kGy. The gels had a stiffening effect, and the rate of relaxation decreased significantly. The water-uptake characteristics of the tensile specimens were investigated; this revealed a decrease in the water absorption tendency with increasing gel content. J Appl Polym Sci 99: 1633–1644, 2006

Key words: electron beam irradiation; injection molding; mechanical properties; nylon; WAXS

INTRODUCTION

The effects of high-energy radiation (electron beams, neutrons, and/or γ rays) on polyamides have been studied by several workers.[1–10] Charlesby[1] was the first to note that high-energy radiation from atomic pile crosslinked polyiminohexamethyleneiminoadipoyl [i.e., polyamide-6,6 (PA66)]. The crosslinking of PA66 by high-energy electrons from resonant transformer-type cathode ray equipment was also observed by Lawton et al.[2] Little[3] reported that pile irradiation of PA66 in air resulted in a rapid loss of strength with a considerable increase in carboxyl end groups. Later studies that used high-energy radiation from atomic piles showed that the primary effect was crosslinking accompanied by a considerable degradation and loss of crystallinity; further, neither crosslinking nor chain scission was proportional to the radiation dose (D).[4–7] In one of the reports,[8] the authors stated that efficient crosslinking of PA66 in the absence of degradation or where degradation was of little or no significance was impossible to attain with straight radiation. The effect of high-energy radiation on several polyamides, including PA66, was also studied by Ueno[9] and Lyons and Glover.[10] However, literature covering the relationship between the structure and the thermal, mechanical, dynamic mechanical, and stress relaxation behaviors of polyamides irradiated by electron beam in air is scanty. Moreover, to the best of our knowledge, high-temperature electron-beam irradiation of polyamides has not been reported so far. In this article, electron-beam irradiation of injection-molded PA66 in air at ambient temperature (303 K) and a high temperature (393 K) is reported.

A further impetus to this work was provided by a recent Japanese report,[11] wherein it was mentioned that efforts were being made to improve the temperature and mechanical characteristics of polyamides by irradiation. In the existing literature on radiation technology, one finds extensive use of tri-

Correspondence to: A. K. Bhowmick (anilkb@rtc.iitkgp.ernet.in).

Contract grant sponsor: Department of Atomic Energy, Board of Research in Nuclear Sciences; contract grant number: Mumbai vide sanction no. 2002/35/7/BRNS/172.

TABLE I
Conditioning of the Tensile and Compression Specimens

Set	Conditioning procedure
X	1. Unannealed specimens were wrapped in Al foil. 2. Wrapped specimens were double-packed in PE packets containing silica gel as the desiccant. 3. Final heat sealing was done to minimize the ingress of moisture. Before any further treatment and/or irradiation, the specimens were removed from the PE packets and then treated accordingly. 4. Irradiation was carried out at room temperature (303 K). 5. Testing was performed immediately after irradiation.
Y	1.–3. These steps were the same as those for Set X. 4. Irradiation was carried out at a high temperature (393 K). 5. Testing was performed immediately after irradiation.
Z	1.–3. These steps were the same as those for Set X. 4. Specimens were dipped in TAC solution and then irradiated at 303 K. 5. Testing was performed immediately after irradiation.
W	1.–4. These steps were the same as those for Set X. 5. The specimens were water-annealed by immersion in boiling water for 12 h. 6. Testing was performed immediately after water annealing.

allyl cyanurate (TAC) and other acrylate monomers, such as ditrimethylolpropane tetraacrylate, trimethylolpropane triacrylate, tetramethylolmethane tetraacrylate, and tripropyleneglycol diacrylate, as commonly used radiation sensitizers.[12–18] The acrylate monomers and TAC are all thermally unstable in the PA66 processing temperature range of 533–573 K. To obviate the processing instability of TAC, some studies have been carried out where TAC was incorporated into PA66 by the dipping of the tensile specimens in a TAC solution. The samples were subsequently irradiated.

In this study, we carried out gel-content studies to determine the relationship between the radiation dosage and extent of crosslinking in PA66. Studies of the structural changes, in terms of percentage crystallinity, were followed by wide-angle X-ray scattering (WAXS) and differential scanning calorimetry (DSC). Changes in the melting temperature (T_m) and crystallization temperature (T_c) were also monitored by DSC. We also studied the mechanical, compressive stress relaxation, and dynamic mechanical properties. To the best of our knowledge, previous studies have not investigated the differences in the compressive stress relaxation behavior of irradiated and unirradiated PA66. Further, from an application viewpoint, compressive stress relaxation experiments are essential.[19] In this investigation, we also studied the water-uptake characteristics of the tensile specimens.

Overall, our objectives in this study were to find out the suitability of electron-beam radiation in the crosslinking of specific industrial PA66 products for use in critical applications related to railways and/or defense and to obtain a fundamental understanding of the structure–property relationships in irradiated and unirradiated PA66.

EXPERIMENTAL

Materials and specimen preparation

A commercial PA66 (Zytel 101L, DuPont, Gurgaon, India) was generously provided by M/s Black Burn & Co. (Mahestala, India); TAC was kindly supplied by M/s NICCO Corp., Ltd. (Shyamnagar, India). Formic acid (85%) was purchased from Ranbaxy Laboratories (S. A. S. Nagar, India) and acetone (extra pure) was procured from E. Merck (Mumbai, India). A 10% (w/w) TAC solution was prepared by the dissolution of TAC in acetone.

The PA66 pellets were dried by dehumidified air at 353 K in a hopper dryer for 6 h before injection molding. A Windsor series injection-molding machine with a screw diameter of 45 mm was used with a screw speed of 50 rpm. The temperatures maintained were 533, 543, and 553 K in the three zones of the molding machine barrel for tensile specimen preparation; 548 K in the nozzle; and 373 K in the mold. The injection pressure was 7 MPa, and the times for injection, cooling, and ejection were 3, 15, and 2 s, respectively. For preparation of the compressive test specimens (cylinders), direct injection molding was done in the same machine. The temperatures maintained were 533, 538, and 543 K in the three zones of the machine barrel and 553 K in the nozzle. The injection pressure was 7.5 MPa, and the times for injection, cooling, and ejection were 40, 30, and 3 s, respectively. Proper precautions for the preservation of the specimens were taken immediately after injection molding to minimize moisture uptake, as mentioned in Table I.

The injection-molded specimens were segregated into sets depending on the conditioning to which the specimens were subjected. These are reported in Table I. The set Z tensile specimens were dipped in 10% TAC solution in acetone for 2 h. The time of dipping

was optimized after experiments were conducted where the variation in TAC uptake was followed gravimetrically with time. This dipping treatment was executed immediately before the irradiation process, which is described in the next section. The compressive test specimens were not subjected to the TAC dipping treatment and were conditioned according to the conditions followed for set X specimens.

Electron-beam irradiation of the molded specimens

Electron-beam irradiation was carried out with a 3-MeV, 150-kW electron accelerator (Dynamitron of RDI, Ridgewood, NY) at NICCO. The irradiation was carried out in air at ambient temperature (303 K) and at a high temperature (393 K). However, the compression test specimens were subjected to ambient-temperature irradiation only.

The specimens were unpacked from the sealed packets and were put on stainless steel trays attached to the conveyor system. The conveyor system (with the capacity to accommodate 65 or more trays) carried the trays to the enclosed room where they passed under the titanium window, through which the electrons of desired energy emerged and impinged upon the specimens kept on the trays. To avoid sample overheating during irradiation, a blower was always on to direct cold air onto the samples passing below the titanium window. D per pass was fixed at 10 kGy. Further, the time taken by any single tray to come back for radiation after it got irradiated once was maintained at 18 min; that is, the frequency of radiation was 18 min. Under the conditions of the experiment, ozone was also formed, and therefore, air was continuously circulated in the radiation chamber to drive off the ozone gas. The penetrability of the electrons in the PA66 molded specimens (the tensile specimens had a maximum thickness of 3.35 mm, and the compression test specimens had a thickness of 12.7 mm) was ensured by the optimization of the beam energy, and the average D was monitored by a cellulose triacetate film dosimeter. For the tensile specimens, single-side radiation was enough, but for the compression test specimens, both-side radiation was used due to their greater thickness. D values of 100, 200, 300, and 500 kGy were used. We carried out the high-temperature irradiation by heating the specimens to the desired temperature of 393 K. After irradiation was over, the specimens were repacked in heat-sealing polyethylene (PE) bags to minimize the ingress of moisture.

The samples were designated as follows: NPQD, where N represents PA66; P represents the type of test specimen, namely, T for tensile test and C for compressive test; Q represents the specimen sets X, Y, Z, and W; and D represents the radiation dose received (kGy). For example, the specimen with the designation NTZ200 represents a tensile specimen of set Z, which received a D of 200 kGy at 303 K. Likewise, the designation NTX0 represents the control tensile specimen of set X, and similarly, the designation NCX500 represents a compressive test specimen belonging to specimen set X, which received 500-kGy D at 303 K.

Gel content

For the evaluation of gel content, portions from the tensile specimens were cut, weighed, and immersed in excess of 85% formic acid. Extraction was continued for 3 days at room temperature; we collected gels by filtering through a fritted glass crucible. The percentage gel content was calculated with the formula

$$\text{Gel content (\%)} = \frac{\text{Unextractable fraction}}{\text{Irradiated specimen weight}} \times 100 \quad (1)$$

The results reported are the average of three measurements from three different portions of each specimen.

To calculate the radiation chemical yield of crosslinking and scission, we used the widely accepted Charlesby–Pinner[20] equation:

$$S + S^{1/2} = (p_0/q_0) + 1/(q_0UD) \quad (2)$$

where S is the sol fraction; p_0 and q_0 are the chain scission and crosslinking density per unit dose (kGy^{-1}), respectively; and U is the number-average degree of polymerization of the polymer before irradiation.

The values of p_0 and q_0 were obtained graphically from the experimental curve of $S + S^{1/2}$ versus $1/D$. The number of polymer chain scissions per 100 eV absorbed [$G(S)$] and the number of polymer crosslink sites per 100 eV absorbed [$G(X)$] are related to p_0 and q_0 by the relation:

$$G(S)/G(X) = 2(p_0/q_0) \quad (3)$$

WAXS characterization

WAXS patterns of the specimens were recorded with a Philips 1710 X-ray diffractometer (Lelyweg, The Netherlands) at room temperature (303 K). The Cu Kα radiation source ($\lambda = 0.154$ nm) was operated at 40 kV and 20 mA. We recorded patterns by monitoring those diffractions that appeared from 15 to 30° (2θ). The scan speed was 0.05°/s. The areas under the crystalline and amorphous portions were determined in arbitrary units, and the percentage crystallinity was calculated with the following equation:

$$\text{Crystallinity (\%)} = I_C \times 100/(I_C + I_A) \quad (4)$$

where I_C and I_A are the integrated intensities corresponding to the crystalline and amorphous phases, respectively. 2θ values were reproduced within a $\pm 0.1°$ variation. The scans were profile-fitted with standard software (ORIGIN 6.0; Microcal Software, Inc., Northampton, MA).

DSC studies

DSC analyses were carried out with a differential scanning calorimeter (model Q 100, TA Instruments–Waters LLC, New Castle, DE) calibrated with indium and sapphire standards. About 10 mg of the polymer samples were weighed out in the aluminum DSC pans for the experiments. All of the specimens were subjected to a ramp heating and ramp cooling procedure under a nitrogen purge of 50 mL/min. In the heating scan, the samples were heated from 303 to 573 K at a heating rate of 10 K/min. The samples were kept for 5 min at this temperature (573 K) to eliminate the previous heat history completely before they were cooled to 303 K at 10 K/min. The thermograms were recorded and analyzed to compare the percentage crystallinity changes and the variation of T_m with increasing D on the basis of the heating scan data. The crystallinity was calculated with the following equation:

$$\text{Crystallinity (\%)} = (\Delta H_{\text{EXP}} \times 100)/\Delta H_F \quad (5)$$

where ΔH_{EXP} is the actual heat of fusion of the sample under study and ΔH_F is the heat of fusion of a 100% crystalline PA66, which was taken to be 190 J/g.[21]

The cooling scan data revealed trends in T_c and heat of crystallization (ΔH_c). The analyses were carried out with Universal Analysis 2000 version 3.9A software (TA Instruments–Waters LLC).

Tensile testing

The injection-molded tensile specimens conforming to type IV of ASTM D 638-98 were tested in a Hounsfield H10KS universal testing machine (Surrey, UK) at a crosshead speed of 50 mm/min at 298 ± 2 K and 50 ± 5% relative humidity. The conditioning history of the tensile dumbbells before testing is presented in Table I. The values reported reflect an average of five measurements. The modulus for the specimens was calculated from the linear portion of the stress–strain graphs.

Compressive stress relaxation studies

The injection-molded compression specimens (cylinders), prepared according to ASTM D 695-96, had a diameter of 12.7 mm and a length of 25.4 mm and conformed to set X of the conditioning procedure, as presented in Table I. Stress relaxation experiments were carried out on a Zwick 1435 universal testing machine (Ulm, Germany) in compression mode. A user-defined compressive strain was applied to the specimen, and the resulting stress was monitored on the digital indicator. Stress relaxation experiments were used to study the deformation characteristics of the polymer on application of a step strain at time $t = 0$. This applied strain energy produced an instantaneous stress (σ_0) in the polymer, and this stress value decreased with time (σ_t). By monitoring the change in the relaxation kinetics, we studied the structural changes induced in the polymer due to radiation.

Dynamic mechanical analysis (DMA) experiments

A DMA 2980 dynamic mechanical analyzer from TA Instruments–Waters LLC was used in dual cantilever mode in the temperature range 303–473 K at a frequency of 1 Hz and a heating rate of 2 K/min. The dimensions of the specimens were 35 × 12.5 × 3.35 mm^3. The data were analyzed with a Universal Analysis 2000 software (version 3.9A, TA Instruments–Waters LLC).

Water absorption

The irradiated specimens were conditioned in an oven for 24 h at 323 ± 2 K and weighed, and then the long-term immersion procedure outlined in ASTM D 570-98 was followed. The immersed specimens were kept in water maintained at 295 K. However, the experiment was discontinued after 42 days. The water-uptake trend after 42 days was calculated with the following equation:

$$\text{Water uptake (\%)} = \frac{(\text{Wet weight} - \text{Conditioned weight})}{\text{Conditioned weight}} \times 100 \quad (6)$$

The values obtained were the average of three readings.

RESULTS AND DISCUSSION

Gel-content measurements

The gel content of the specimens is tabulated in Table II. In each specimen set, the gel content increased with D. The highest gel content was obtained for NTZ500, whereas NTX0 and NTW0 had no gels. The presence of TAC increased the gel content at D values of 200 and 500 kGy over those specimens that were not TAC-

TABLE II
Gel Content of the Irradiated PA66 Specimens

Sample designation	Gel content (%)[a]
NTX0	—
NTX200	3.5 (0.2)
NTX300	11.1 (0.2)
NTX500	22.0 (0.4)
NTY100	1.3 (0.2)
NTY200	6.8 (0.3)
NTY500	24.5 (0.5)
NTZ100	1.5 (0.1)
NTZ200	7.0 (0.3)
NTZ500	28.0 (0.3)
NTW0	—
NTW200	5.0 (0.3)
NTW300	14.1 (0.3)
NTW500	26.0 (0.3)

[a] The numbers in parentheses indicate the standard deviations based on three measurements.

treated but received the same D at ambient temperature. The increase in the gel content of the high-temperature irradiated specimens over the ambient-temperature irradiated specimens proved that it probably followed the laws of chemical kinetics, as both crosslinking and chain scission reactions would be accelerated with increasing temperature. However, the slight improvement in the gel content of NTY500 over NTX500 proved that there were more chain scissions than crosslinking in the former. The water-annealed specimens showed an increase in gel content over the set X specimens. From the gel-content values, the following trend of comparative increase (from left to right) in chain crosslinking was evident: PA66 radiated at 303 K $<$ PA66 radiated at 393 K $\approx$ PA66 radiated at 303 K and water annealed at 373 K $<$ TAC-treated PA66 radiated at 303 K.

The reason for the increase in crosslinking tendency with increasing temperature of irradiation may have been due to the enhanced mobility of the PA66 molecules above the glass-transition temperature (T_g). Because of the greater number of chain segmental movements at a temperature of 393 K, crosslink formation was easier than when the chains were more frigid (at 298 K, which was much below the T_g of PA66). Charlesby–Pinner plots of specimen sets X, Y, and W were made. Two representative plots for sets X and W are shown in Figures 1(a) and 1(b), respectively. The p_0/q_0 values obtained from the plots are tabulated along with their corresponding $G(S)/G(X)$ values in Table III. The p_0/q_0 values were obtained by linear curve fitting with ORIGIN 6.0. On the whole, $G(S)/G(X)$ values of 3.0, 3.2, and 2.8 were on the higher side ($>$1.0), which implied that the scission probability for air-irradiated PA66 was relatively high. Lyons and Glover[10] reported $G(S)/G(X)$ values of 1.2–1.4 for PA66 irradiated under a nitrogen atmosphere. However, Schnabel[22] reported a $G(S)/G(X)$ value of 3.4 for the room-temperature irradiation of PA66. In a previous study[23] on compression-molded PA66 thin films, we found the $G(S)/G(X)$ value to be 3.3 for room-temperature electron-beam irradiation.

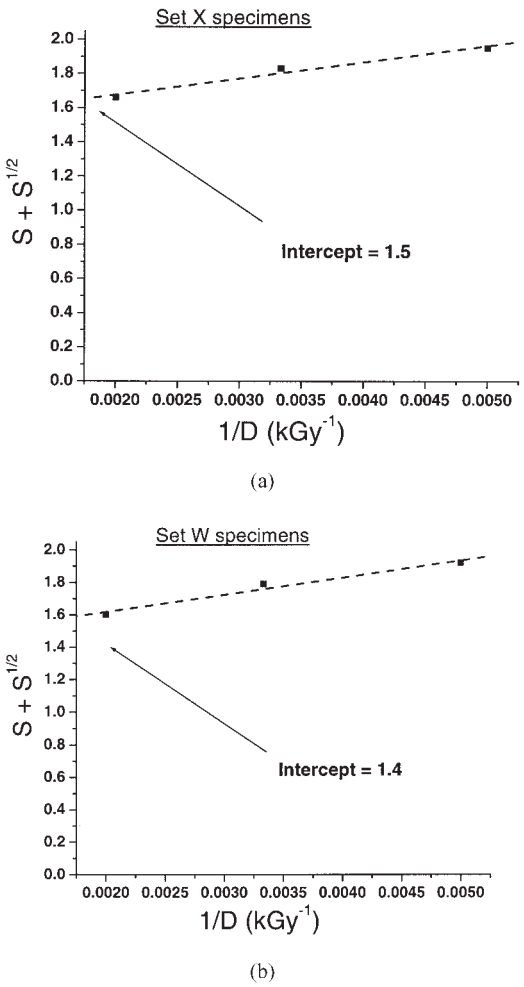

Figure 1 Charlesby–Pinner plots for specimens of sets (a) X and (b) W.

This variation in $G(S)/G(X)$ values can be explained on the basis of radiolytic oxidation and also the chain scissioning tendency during the radiation process. All of the tests except water absorption were carried out within 5 days of the radiation date to minimize postirradiation oxidation. Previous researchers[10] annealed

TABLE III
***G(S)/G(X)* Values for Set X, Y, and W Tensile Specimens from the p_0/q_0 Values as Obtained from Charlesby–Pinner Plots**

Serial No.	Particulars	p_0/q_0	$G(S)/G(X)$
1	Set X specimens	1.5	3.0
2	Set Y specimens	1.6	3.2
3	Set W specimens	1.4	2.8

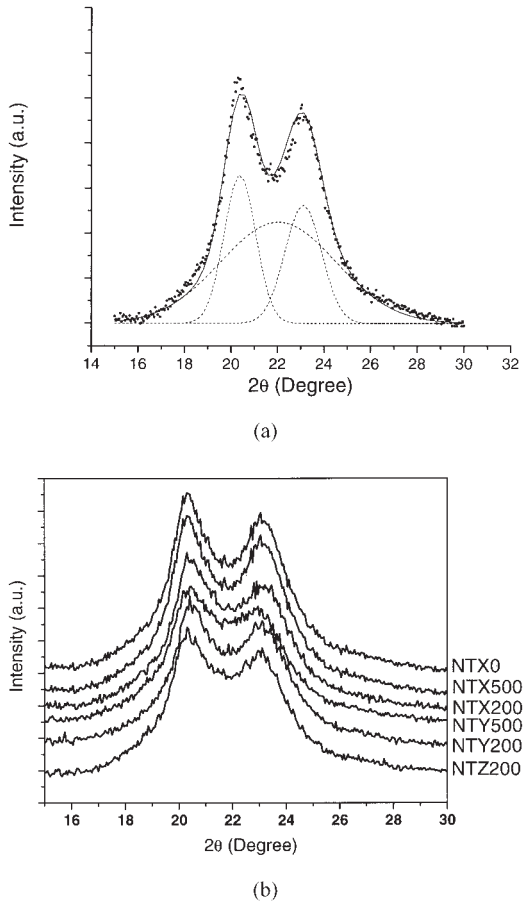

Figure 2 (a) Example of the profile analysis of the diffraction scan of NTX0 and (b) WAXS profiles of some of the PA66 specimens (as indicated next to each curve) obtained at various *D* values. The curves are vertically offset for clarity.

PA66 in a nitrogen atmosphere for 30 min at 448 K immediately after irradiation to remove trapped free radicals and, thereby, prevented postirradiation oxidation from influencing the polymer response. However, in industrial practice, such elaborate methods of annealing are generally not present. We resorted to the boiling-water annealing technique on injection-molded PA66 specimens to relieve internal stresses and to provide a comparable thermal history and equivalent moisture content. The $G(S)/G(X)$ value for the specimens belonging to set W was 2.8, which was slightly less than the value of 3.0 obtained for the set X specimens. It is known that the reactive species generated within an irradiated polymer may remain unchanged for days, weeks, or longer at room temperature.[24] By annealing, these reactive species (those residing in the amorphous regions) can be made to react with the polymer chains, thereby preventing their reaction with oxygen diffusing into the polymer. At the high temperature of 448 K used by Lyons and Glovers, probably most of the reactive species underwent reactions with the polymer, which thereby increased the gel content and, hence, led to a lower value of $G(S)/G(X)$. Similarly, when the set X specimens were annealed in boiling water, the gel content increased, and also, the $G(S)/G(X)$ value decreased. So, water annealing proved to be beneficial in increasing the gel content after the initial irradiation process. However, in this study, air was the ambient circulating medium during radiation, unlike nitrogen gas (nonoxidizing nature), which was used by Lyons and Glover during irradiation.

WAXS results

WAXS was used to investigate the changes in crystalline structure that resulted from electron-beam irradiation. The experimental diffractometer scans were profile-fitted, and an example of the profile analysis with the scan for NTX0 is shown in Figure 2(a). Here, the filled circles are the observed data points, the peaks shown in broken curves are the resolved components, and the full line through these data points was derived from profile analysis and is the sum of the various component peaks. The diffraction curve of PA66 could be deconvoluted into three components (one amorphous and two crystalline) by the approximation of the peaks with Gaussian curves.[25] The two most intense reflections in the WAXS pattern from PA66 are (100) and (010) + (110), which occurred at 2θ values of about 20.4 and 23.1°, respectively, for Cu Kα radiation. In our previous study[23] on compression-molded PA66 thin films, these characteristic 2θ values occurred at 20.2 and 23.8°, respectively. These corresponded to the $\alpha 1$ and $\alpha 2$ peaks. However, apart from these $\alpha 1$ and $\alpha 2$ peaks, two other peaks occurring at 13.5 and 22.3° were seen and were designated as $\gamma 1$ and $\gamma 2$, respectively. However, in injection-molded PA66 specimens, no γ peaks were found. The variations in 2θ and the corresponding *d*-spacing (interplanar distance) values were negligible with *D* and, hence, are not reported here. The WAXS diffractograms for these tensile specimens are shown in Figure 2(b). The crystal structures usually observed at room temperature in PA66 are the α and β form,[26] the α form being the most commonly occurring phase. The nonoccurrence of peak intensities at 2θ values of about

TABLE IV
Percentage Crystallinity of the PA66 Specimens as Obtained from WAXS

Sample code	Crystallinity (%)
NTX0 (control)	44
NTX200	42
NTX500	39
NTY200	40
NTY500	37
NTZ200	41

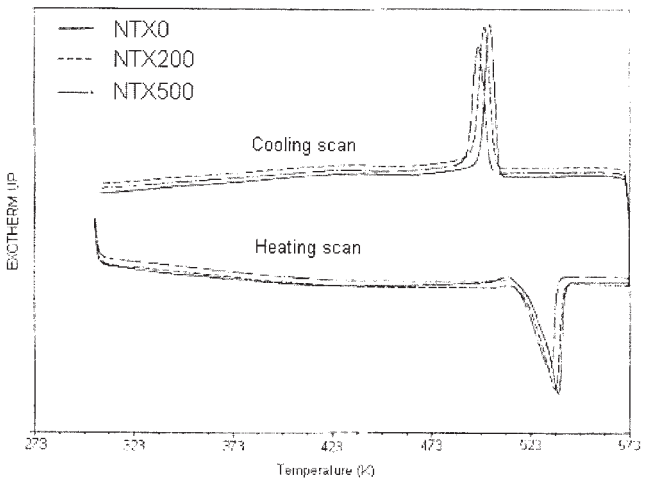

Figure 3 Comparison of DSC thermograms of NTX0, NTX200, and NTX500 showing the heating and cooling scans.

12 and 19° confirmed the absence of the β form in the injection-molded specimens.

The percentage crystallinity of the specimens is presented in Table IV. It was evident that the crystallinity slightly decreased with increasing D. High-temperature irradiation of the specimens (NTY200 and NTY500) resulted in a further loss in crystallinity over the specimens receiving the same D but irradiated at room temperature. The crystalline content of the TAC-treated specimens was between those of the ambient-temperature irradiated and high-temperature irradiated neat PA66 specimens.

DSC results

It is well known that the thermodynamics of melting and crystallization are influenced by crosslinking and chain scission. The DSC heating and cooling runs for some of the specimens belonging to sets X, Y, and Z were done, and a representative plot for the set X specimens is shown in Figure 3. The results for the heating and cooling scans are tabulated in Table V. The observed T_m of about 537 K for the control (NTX0) was within the range specified in the literature.[27] The depression of T_m was marginal, although clearly distinct, as shown in Table V. The heating runs for the specimens showed the melting endotherms in the as-received condition. Because the previous thermal history of a polymer affects its measured degree of crystallinity, these samples were evaluated both as received and after they were subjected to a thermal treatment (holding at 573 K for 5 min, as mentioned in the Experimental section) designed to give an equivalent thermal history to all of the PA66 samples. The trend in the percentage crystallinity data received from the first heating run as reported in Table V was in consonance with that obtained from WAXS studies, where the samples subjected to different thermal and processing histories were evaluated as such to gain insight into the crystallinity (structural) changes. The crystallinity decreased with increasing D. Further, for the neat specimens, the percentage crystallinity at any specific dose was lower when the irradiation was carried out at an elevated temperature compared to when it was carried out at ambient temperature. The later values were, however, comparable with the TAC-dipped specimens irradiated at ambient temperature. The crystallinity trend from DSC mirrored the trend observed from the WAXS of the specimens. The decrease in the ΔH_{EXP} for the TAC-dipped specimens compared to the neat specimens irradiated at ambient temperature revealed that some sort of interaction took place between the TAC molecules and the PA66 chains. This interaction most probably led to an inhibition of crystalline growth in PA66. A similar phenomenon was previously observed in the *N,N′*-bismaleimide-4,4′-biphenylmethane/polyamide-10,10 system.[28]

Other researchers[29,30] previously studied the radiation-induced changes of crystallinity in polymers and related the molar fraction (x) of the crystalline units after irradiation to values of the melting temperature before irradiation ($T_{m,0}$) and the melting temperature after irradiation ($T_{m,d}$), according to an equation derived by Flory:[31]

$$(1/T_{m,d}) - (1/T_{m,0}) = (R\ln x/\Delta H) \qquad (7)$$

where R and ΔH denote the universal gas constant and the enthalpy of fusion per mole of crystalline units for the polymer under study, respectively. Both $T_{m,0}$ and $T_{m,d}$ are expressed in the Kelvin scale of temperature. The number of crystalline units excluded from the crystal per 100 eV of absorbed energy (G) can be calculated according to

TABLE V
T_m, ΔH_{EXP}, and Percentage Crystallinity from the DSC Heating Scan and T_c and ΔH_c from the DSC Cooling Scan of the PA66 Tensile Specimens

Sample code	T_m (K)	ΔH_{EXP} (J/g)	Crystallinity (%)	T_c (K)	ΔH_c (J/g)
NTX0	537	70	37	503	63
NTX200	535	67	35	500	62
NTX500	532	61	32	497	59
NTY200	534	65	34	498	61
NTY500	530	58	31	495	57
NTZ200	534	65	34	498	61
NTZ500	532	59	31	497	58
NTW0	537	69	36	501	63
NTW200	535	64	34	500	58
NTW500	530	59	31	496	56

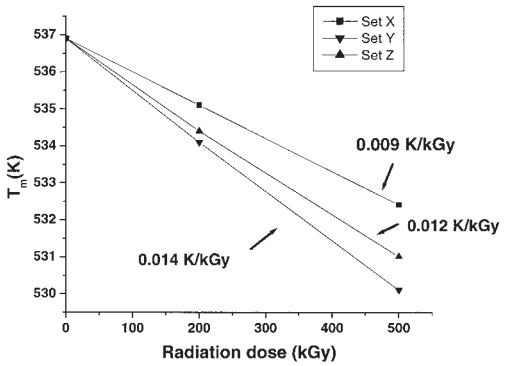

Figure 4 Depression of T_m of sets X, Y, and Z of PA66 with D.

$$G = (1 - x)(100N_A)/(MD) \quad (8)$$

where N_A is Avogadro's number ($\sim 6 \times 10^{23}$), D is the absorbed dose in eV/g, and M is the molecular unit of the repeat unit along the c axis of the crystalline unit.

Kusy and Turner[30] studied radiation-induced changes in T_m of degassed PA66 irradiated *in vacuo* by ^{60}Co γ rays at a temperature of about 313 K by DSC. From their study, they concluded that T_m decreased linearly with absorbed D, and a straight line drawn through their data obtained for the first DSC heating runs indicated the depression of the T_m to be 0.009 K/kGy. An estimate of the number of radiation-damaged crystalline units yielded a G value of 9. A recalculation of the G value of Kusy and Turner based on the values of R and ΔH as 8.314 J K^{-1} mol^{-1} and 190 J/g (instead of the value of ΔH = 207 J/g as used by Kusy and Turner), respectively, yielded a value of G of 10.4. A similar treatment of the data obtained from this study is plotted in Figure 4. The depressions of the T_m for the set X, Y, and Z specimens were 0.009, 0.014, and 0.012 K/kGy, respectively, and the G values for sets X, Y, and Z were 7.1, 10.6, and 8.8, respectively. With high-temperature radiation, the amount of crystalline units excluded from the crystals was higher compared to that for the specimens irradiated at room temperature. The specimens of set Z, which were dipped in TAC, also showed a higher extent of crystal-unit exclusion than the set X specimens.

The results from the DSC cooling scans reveal that with increasing D, the crystallization was progressively inhibited such that T_c shifted to lower temperatures and the value of ΔH_c also decreased. For high-temperature radiation, the corresponding decrease was more than that for the ambient-temperature radiation at equivalent doses. It is well known that both chain scission and crosslinking reactions lead to loss in the degree of crystallinity (measurable from the ΔH_c values) and a decrease in T_c. Further, the decreases in both T_c and ΔH_c were more in the specimens treated with TAC than in their neat counterparts. So a similar trend was noticed from the DSC crystallization and melting studies that matched the trend from the WAXS data.

The DSC data for the heating and cooling scans for NTW0, NTW200, and NTW500 are reported in Table V. A comparison of the previous values for set W specimens with those of the set X specimens revealed that the trend of decreasing crystallinity with increasing D was also repeated here.

Tensile behavior

The yield strength (YS), tensile modulus, and elongation at break (EB) are compared for sets X, Y, and Z in Table VI. The maximum improvement in YS occurred for the specimen irradiated at 200 kGy at ambient temperature (viz., NTX200) and was about 10.0% over the control. The improvement in YS of NTX100 was 7.0%, whereas the values for NTX300 and NTX500 over the control were 4.0 and 2.0%, respectively. This very similar trend was reflected in the specimen sets Y and Z. However, the overall improvement in YS in these sets at comparable Ds was less than that observed for the specimens belonging to set X. This was quite contradictory to the gel-content data. This could be explained only on the basis of a loss of crystallinity on radiation, as shown previously by the WAXS and DSC studies. In semicrystalline polymers such as PA66, crystallinity plays a pivotal role in shaping the tensile properties, and so a loss of crystallinity (and, hence, an increase in amorphousness) on radiation would have a major impact on tensile behavior. Moreover, under the experimental conditions during the radiation process, radiolytic oxidation due to oxygen and ozone was evident, as mentioned in the discussion on gel content.

Radiolytic decomposition can be accelerated and retarded by the presence of oxygen. PE, polypropylene, and polystyrene are predominantly degraded

TABLE VI
YS, Tensile Modulus, and EB for the Specimen Sets X, Y, and Z

Sample code	YS (MPa)	Modulus (GPa)	EB (%)
NTX0	76.9 (1.0)	2.45 (0.21)	63 (6)
NTX100	82.3 (0.8)	2.83 (0.18)	68 (4)
NTX200	84.5 (0.6)	2.92 (0.16)	70 (7)
NTX300	80.0 (0.7)	2.74 (0.11)	55 (3)
NTX500	78.3 (0.5)	2.66 (0.14)	48 (4)
NTY200	80.9 (0.8)	2.79 (0.15)	36 (6)
NTY500	77.3 (0.4)	2.63 (0.17)	28 (3)
NTZ200	81.5 (0.6)	2.79 (0.11)	44 (4)
NTZ500	79.1 (0.5)	2.68 (0.15)	38 (3)

The numbers in parentheses indicate the standard deviations based on five measurements.

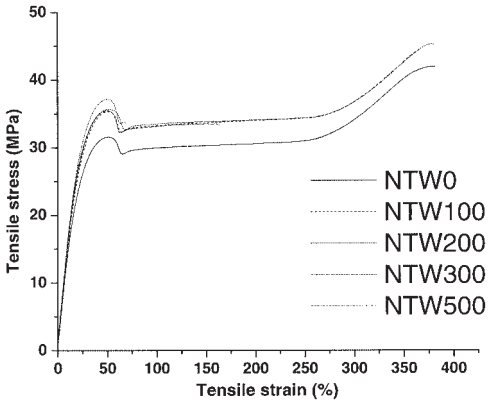

Figure 5 Tensile stress–tensile strain curves for set W specimens.

in the presence of air (and, hence, oxygen) if the dose rate is low enough, whereas the degradation of poly(methyl methacrylate) is protected by oxygen.[32] We believe that the presence of dissolved oxygen in the PA66 specimens substantially influences the tensile results. Moreover, after the oxygen, which is initially dissolved in the sample, is used up, the diffusion of oxygen from the sample surface affects the response of the polymer to radiation-induced changes. This diffusion of oxygen into the bulk of the specimen is also dependent on the ambient temperature and the thickness of the specimen. If the oxygen diffusion rate is comparable to the rate of oxygen consumption, oxidative processes can proceed. Experimental results published for PE and polypropylene[32] support the previous viewpoint when the *D* rate used was low. In this study, the probability of oxygen and/or ozone diffusion as the radiation continued could not be ruled out at the dose rate of 10 kGy. Also, a long loop time of the conveyor to bring the sample again under the beam may have allowed ingress of oxygen. An optimization probably occurred at the 200-kGy *D,* where the YS, tensile modulus, and EB were significantly higher than that of the control. We can explain the increase in EB for NTX100 and NTX200 over NTX0 by considering the plasticizing action of the degradation products produced in the polymer at these low *D* values.[33] It is known that the result of oxidative attacks is usually peroxides and hydroperoxides, which would promote scission and other main chain breaking reactions and lead to a decrease in the average molecular weight of the polymer, which would eventually lead to a decrease in the tensile values. So, at higher *D* values, the YS values decreased.

For the elevated temperature radiations in air, the oxygen diffusion process would be enhanced according to the principles of chemical kinetics, even though the crosslinking and chain scissioning tendency would also probably increase at such an elevated temperature (393 K). The PA66 polymer chains were not frigid above T_g (≈333–353 K). The increase in YS and tensile modulus for all of the irradiated specimens indicated the formation of a network structure in PA66, which was further corroborated by the gel-content results. However, as shown in Table III, the $G(S)/G(X)$ value was 3.2 for the high-temperature radiated specimens compared to 3.0 for the ambient-temperature radiated specimens. This hinted at relatively more chain scission reactions at higher temperatures, which explained the fall in modulus values for the specimens of set Y. The $G(S)/G(X)$ value of 3.1 for the set Z specimens also hinted at more of chain scission events than crosslinking events and, hence, a similar trend in modulus. The results in Table VI can be explained by the previous propositions.

To remove frozen-in stresses in injection-molded PA66 specimens and also to provide an equivalent moisture content, the tensile specimens belonging to specimen set W were water annealed. The tensile stress–tensile strain plots for these specimens are shown in Figure 5. The variation in YS, ultimate tensile strength (UTS), EB, and 10% modulus is shown in Figure 6. The YS, UTS, and modulus values were less than those for the specimens that were not water annealed, as it is known that water acts as a plasticizer in PA66 and, thereby, increases the EB and, at the same time, reduces the tensile strength. The YS values of all of the water-annealed irradiated specimens were higher than that of the unirradiated water-annealed specimen. The 10% modulus values also followed a similar trend to that of YS. This provided evidence of crosslinking in the irradiated specimens. Both YS and 10% modulus values went through a maximum and

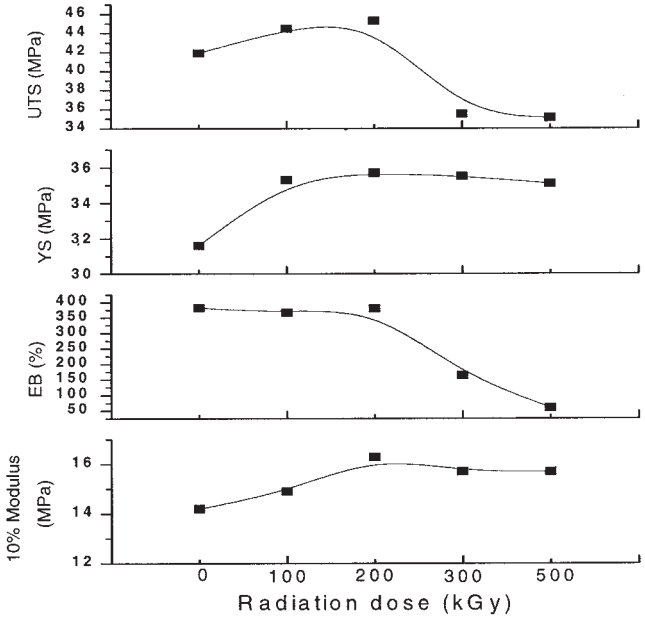

Figure 6 Variation in YS, UTS, EB, and 10% modulus for the specimens belonging to set W.

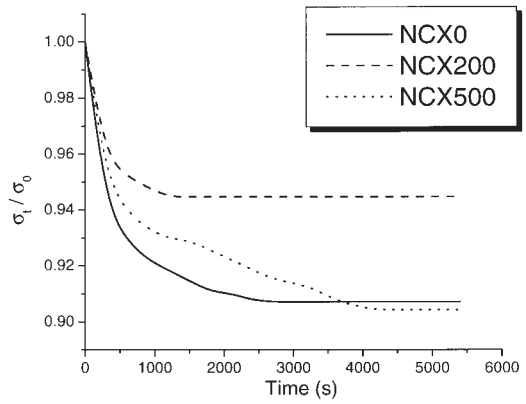

Figure 7 σ_t/σ_0 versus time for some of the compressive test cylinders belonging to set X.

then nearly leveled off. This provided evidence for increased chain scissions/radiolytic oxidations beyond a *D* of 200 kGy. The EB value of NTW200 was slightly greater than that of NTW100 but was slightly less than that of NTW0 (control). This can be probably explained on the basis of the release of frozen-in stress introduced during injection molding and structural rearrangements of loosely formed oxidative reaction products as a result of boiling water annealing. However, a general trend of EB decreasing with increasing *D* was observed in this system. The effect of crosslinking on a polymer is to increase its tensile strength, initially. However, the increased crosslinking also reduces the ultimate elongation so that at higher degrees of crosslinking, the tensile strength decreases again. So, from a practical viewpoint, the specimen radiated to a dose of 200 kGy and subsequently annealed by boiling water showed the optimization of tensile properties.

Compressive stress relaxation

The stress relaxation data are shown in terms of the dimensionless ratio σ_t/σ_0 versus time in Figure 7 for an applied compressive strain of 2%. This is the first report on such systems. Here, σ_t represents the stress at time *t* and σ_0 represents the stress value at the start of the experiment. As usual, the ratio σ_t/σ_0 exponentially decreased with time. The decrease was much faster with the unmodified samples. Also, σ_t/σ_0 reached an equilibrium value of 0.94 for the modified samples (NCX200) compared to a value of about 0.91 for the unmodified one (NCX0). It was clear that by electron-beam modification, the stress retention was much better with the modified samples. It is well known that both gels and high molecular weights have a stiffening effect on the relaxation modulus, and these reduce the rate of relaxation quite markedly, which results in slower stress relaxation. On the other hand, low-molecular-weight and low-gel samples increase the rate of relaxation.[34] Because the control sample had no gel, it showed a faster rate of relaxation compared to the 200-kGy irradiated sample, but it took a longer time than NCX200 to reach the equilibrium stress ratio value due to its higher crystallinity level. It is known that a slower rate of relaxation corresponds to a more elastic or solid-like material.[35] However, we were surprised to find that even though NCX500 had a higher gel content than NCX200, it showed a lower equilibrium stress ratio value at a similar compressive strain over the time range studied. Here, the effect of crystallinity and chain scission also played a major role in shaping the sample relaxation behavior.

DMA studies

The variations in tan δ and storage modulus (*E′*) with temperature are shown in Figure 8(a) for the specimens belonging to set X. Figure 8(a) shows a marginal tan δ peak shift toward higher temperature with in-

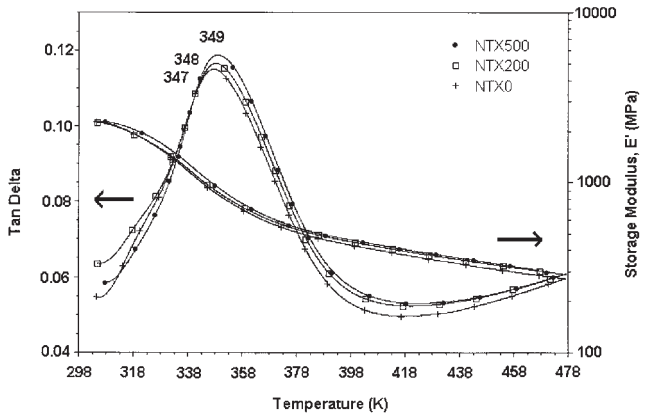

(a)

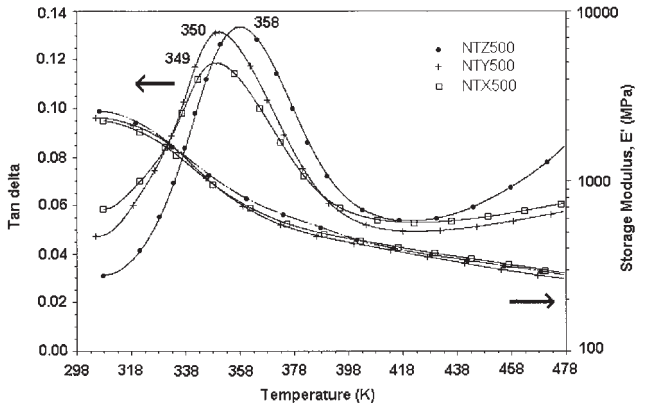

(b)

Figure 8 (a) Tan δ and *E′* versus temperature curves for (a) NTX0, NTX200, and NTX500 and (b) NTZ500, NTY500, and NTX500.

creasing D. The T_g values for NTX0, NTX200, and NTX500 were 347, 348, and 349 K, respectively. The T_g values were very close and, hence, within experimental error. The tan δ peak heights also increased with increasing D, possibly due to the decrease in crystallinity. The E' curve for NTX500 was slightly higher than the E' curve for NTX200, which in turn, was higher than that of the control (NTX0). In semicrystalline crosslinked polymers such as PA66, the residual crystallinity in the polymer and the gel play important roles in shaping the E' curves. Because in the radiated specimens (NTX200 and NTX500) the residual crystallinity was lower than that in NTX0, the E' curves should have shown the reverse trend. However, if the crosslinking effect is taken into consideration as evidenced from gel-content studies, the trend seen in Figure 8(a) is justified. A complex interplay of crystallinity, crosslinking, and radiolytic oxidation/degradation was responsible for the differences in the E' curves.

In Figure 8(b), the tan δ and E' variations are compared for NTZ500, NTY500, and NTX500. The T_g values were 358, 350, and 349 K, respectively. This proved that there was increased crosslinking from specimens X to Y to Z. However, as shown by the E' curves, the E' for NTY500 went below that of NTX500 at about 348 K, whereas that of NTZ500 dipped below that of NTX500 at about 398 K. This was explained on the basis of the inherently weaker structures in NTZ500 and NTY500 due to more chain scissions than that occurred in NTX500. This validated our modulus trends for the specimens receiving a 500-kGy dose, as shown in Table VI.

Water-uptake characteristics

The water-uptake characteristics of the injection-molded PA66 specimens were studied to check for any improvement in the water absorption resistance as a result of radiation-induced crosslinking. The water-uptake behavior of NTX0 was compared with the specimens receiving a 200- and 500-kGy D from each of the specimen sets X, Y, and Z, as shown in Figure 9. The control specimen of set X, which also served as the control for all of the other specimen sets, showed the maximum amount of water absorption after 42 days. The following trend, which is shown in Figure 9, NTX0 > NTX200 > NTX500 > NTZ200 > NTZ500 > NTY200 > NTY500, implied that the water absorbing tendency progressively decreased from NTX0 to NTY500 due to the following factors: (1) increasing D at a fixed temperature, (2) increasing temperature of radiation at a fixed dose, and (3) the presence of TAC. All of these factors were also pertinent for the gel-content and crystallinity trends. So, it was evident that the influence of gel content and residual crystallinity shaped the water-absorbing tendency in the injection-molded PA66 specimens.

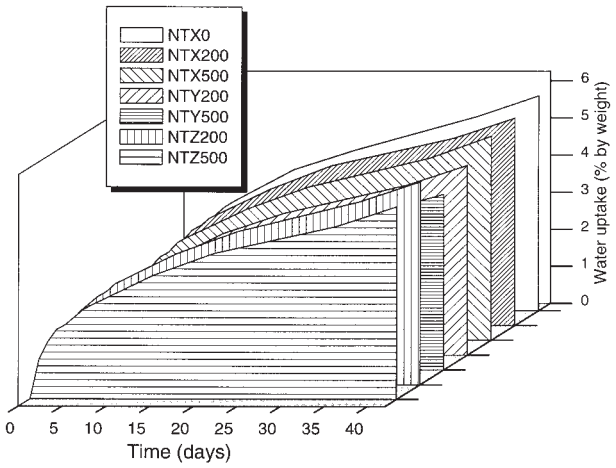

Figure 9 Water uptake versus time for NTX0, NTX200, NTX500, NTY200, NTY500, NTZ200, and NTZ500.

CONCLUSIONS

In this study, tensile test and compressive test specimens were prepared by the injection molding of PA66 to explore the effects of electron-beam irradiation in air. The crystalline structure and variations in crystalline levels were investigated with the following variables: D at ambient and high temperatures and TAC treatment followed by radiation at ambient temperature. Crystallinity decreased with electron-beam irradiation in air. The gel content increased with electron-beam dose, with the increase being higher for TAC-treated samples and when the higher irradiation temperature was used. The loss in crystalline units in terms of G value was determined from DSC analyses and was dependent on the previous variables. The role of radiolytic oxidation in decreasing the gel-content values was discussed. Water annealing as a postirradiation technique was demonstrated, probably for the first time, to increase the gel content. From the tensile strength and compressive stress relaxation behavior, a 200-kGy D was chosen as the preferred dose limit. DMA and gel-content studies also supported the results obtained from the stress relaxation experiments. The DMA and water absorption behaviors of the specimens showed that the 200-kGy D was the preferred one. The notable achievement of this study was that the tensile strength, modulus, compressive stress relaxation behavior, and water absorption tendencies of pristine PA66 improved without the use of any filler, which would definitely lead to savings in terms of product weight and cost.

References

1. Charlesby, A. Nature 1953, 171, 167.
2. Lawton, E. J.; Bueche, A. M.; Balwit, J. S. Nature 1953, 172, 76.

3. Little, K. Nature 1954, 173, 680.
4. Deeley, C. W.; Woodward, A. E.; Sauer, J. A. J Appl Phys 1957, 28, 1124.
5. Valentine, L. J Polym Sci 1957, 23, 297.
6. Zimmerman, J. J Appl Polym Sci 1959, 2, 181.
7. Zimmerman, J. J Polym Sci 1960, 46, 151.
8. Bernstein, B. S.; Odian, G.; Orban, G.; Tirelli, S. J Polym Sci Part A: Gen Pap 1965, 3, 3405.
9. Ueno, K. Radiat Phys Chem 1990, 35, 126.
10. Lyons, B. J.; Glover, L. C., Jr. Radiat Phys Chem 1990, 35, 139.
11. Mizusawa, K.; Baba, T. Nucl Instr Methods Phys Res Sect B 2003, 208, 106.
12. Chaki, T. K.; Roy, S.; Despande, R. S.; Majali, A. B.; Tikku, V. K.; Bhowmick, A. K. J Appl Polym Sci 1994, 53, 141.
13. Tikku, V. K.; Biswas, G.; Despande, R. S.; Majali, A. B.; Chaki, T. K.; Bhowmick, A. K. Radiat Phys Chem 1995, 45, 829.
14. Datta, S. K.; Bhowmick, A. K.; Chaki, T. K.; Majali, A. B.; Despande, R. S. Polymer 1996, 37, 45.
15. Sen Majumder, P.; Bhowmick, A. K. J Adhes Sci Technol 1998, 12, 831.
16. Sen Majumder, P.; Bhowmick, A. K. Wear 1998, 221, 15.
17. Banik, I.; Dutta, S. K.; Chaki, T. K.; Bhowmick, A. K. Polymer 1999, 40, 447.
18. Chattopadhyay, S.; Chaki, T. K.; Bhowmick, A. K. J Appl Polym Sci 2001, 79, 1877.
19. Sengupta, R.; Tikku, V. K.; Somani, A. K.; Chaki, T. K.; Bhowmick, A. K. Unpublished manuscript.
20. Charlesby, A.; Pinner, S. H. Proc R Soc Ser A 1959, 249, 367.
21. Thermal Characterization of Polymeric Materials, 2nd ed.; Turi, E. A., Ed.; Academic: San Diego, 1997; p 2026.
22. Schnabel, W. In Aspects of Degradation and Stabilization of Polymers; Jellinek, H. H. G., Ed.; Elsevier Scientific: Amsterdam, 1978; p 162.
23. Sengupta, R.; Tikku, V. K.; Somani, A. K.; Chaki, T. K.; Bhowmick, A. K. Radiat Phys Chem 2004, 72, 625.
24. Clough, R. In Encyclopedia of Polymer Science and Engineering; Mark, H. F.; Bikales, N. M.; Overberger, C. G.; Menges, G., Eds.; Wiley: New York, 1998; Vol. 13; p 667.
25. Clark, E. S.; Wilson, F. C. In Nylon Plastics; Kohan, M. I., Ed.; Wiley-Interscience: New York, 1973; Chapter 8.
26. Jain, A.; Vijayan, K. J Mater Sci 2002, 37, 2623.
27. ASTM D 4066, Standard Classification System for Nylon Injection and Extrusion Materials; ASTM International: West Conshohocken, PA, 2000.
28. Zhang, L.; Zhang, H.; Chen, D. Radiat Phys Chem 1999, 56, 323.
29. Dole, M.; Howard, W. H. J Phys Chem 1957, 61, 137.
30. Kusy, R. P.; Turner, D. T. Macromolecules 1971, 4, 337.
31. Schnabel, W. In Aspects of Degradation and Stabilization of Polymers; Jellinek, H. H. G., Ed.; Elsevier Scientific: Amsterdam, 1978; p 176.
32. Schnabel, W. In Aspects of Degradation and Stabilization of Polymers; Jellinek, H. H. G., Ed.; Elsevier Scientific: Amsterdam, 1978; p 169.
33. Makhlis, F. A. Radiation Physics and Chemistry of Polymers; Elsevier Scientific: New York, 1975; p 192.
34. Bhowmick, A. K.; Cho, J.; MacArthur, A.; McIntyre, D. Polymer 1986, 27, 1889.
35. Bhatt, C. U.; Royer, J. R.; Hwang, C. R.; Khan, S. A. J Polym Sc Part B: Polym Phys 1999, 37, 1045.